Available online at www.sciencedirect.com
SCIENCE DIRECT
Biochemical Pharmacology 70 (2005) 134–143
Biochemical Pharmacology
www.elsevier.com/locate/biochempharm

Inhibition of dipeptidyl-peptidase IV catalyzed peptide truncation by Vildagliptin ((2S)-{[(3-hydroxyadamantan-1-yl)amino]acetyl}-pyrrolidine-2-carbonitrile)

Inger Brandt [a], Jurgen Joossens [b], Xin Chen [c], Marie-Berthe Maes [a], Simon Scharpé [a], Ingrid De Meester [a], Anne-Marie Lambeir [a,*]

[a] *Laboratory of Medical Biochemistry, Department of Pharmaceutical Sciences, University of Antwerp, Drie Eiken Campus, Universiteitsplein 1 building S6 B-2610 Antwerpen (Wilrijk), Belgium*
[b] *Laboratory of Medicinal Chemistry, Department of Pharmaceutical Sciences, University of Antwerp, Universiteitsplein 1, B-2610 Antwerp, Belgium*
[c] *Division of Biotechnology and Pharmaceutical Research, National Health Research Institutes, Nankang, Taipei, Taiwan, ROC*

Received 25 February 2005; accepted 14 April 2005

Abstract

Vildagliptin (NVP-LAF237/(2S)-{[(3-hydroxyadamantan-1-yl)amino]acetyl}-pyrrolidine-2-carbonitrile) was described as a potent, selective and orally bio-available dipeptidyl-peptidase IV (DPP IV, EC 3.4.14.5) inhibitor [Villhauer EB, Brinkman JA, Naderi GB, Burkey BF, Dunning BE, Prasad K, et al.1-[[(3-Hydroxy-1-adamantyl)amino]acetyl]-2-cyano-(S)-pyrrolidine: a potent, selective, and orally bioavailable dipeptidyl peptidase IV inhibitor with antihyperglycemic properties. J Med Chem 2003;46:2774–89]. Phase III clinical trials for the use of this compound in the treatment of Type 2 diabetes were started in the first quarter of 2004. In this paper, we report on (1) the kinetics of binding, (2) the type of inhibition, (3) the selectivity with respect to other peptidases, and (4) the inhibitory potency on the DPP IV catalyzed degradation of glucagon-like peptide-1 (GLP-1), glucose-dependent insulinotropic polypeptide (GIP) and substance P. Vildagliptin behaved as a slow-binding DPP IV inhibitor with an association rate constant of 1.4×10^5 M^{-1} s^{-1} and a K_i of 17 nM. It is a micromolar inhibitor for dipeptidyl-peptidase 8 and does not significantly inhibit dipeptidyl-peptidase II (EC 3.4.11.2), prolyl oligopeptidase (EC 3.4.21.26), aminopeptidase P (EC 3.4.11.9) or aminopeptidase M (EC 3.4.11.2). There was no evidence for substrate specific inhibition of DPP IV by Vildagliptin or for important allosteric factors affecting the inhibition constant in presence of GIP and GLP-1.

Keywords: Dipeptidyl-peptidase IV; LAF237; GLP-1; GIP; Substance P; Protease inhibitor

1. Introduction

Dipeptidyl-peptidase IV/CD26 (DPP IV/CD26; EC 3.4.14.5) belongs to the prolyl oligopeptidase family of serine proteases. It cleaves off the N-terminal dipeptide from peptides with proline or alanine in the second position. Although DPP IV is an extracellular membrane protein it is also found in human plasma in a soluble form lacking the transmembrane region. The expression of DPP IV on the surface of differentiated cell types in endothelia, epithelia, and the hematopoietic system has been reviewed [1].

The disease cluster known as the 'metabolic syndrome' comprises a number of disorders including type 2 diabetes, arterial hypertension, dyslipidemia and obesity. The current treatments of type 2 diabetes are unsatisfactory in terms of prevention of complications and preservation of quality of life. The sulfonylureas and the newer class of glinides (e.g. repaglinide) both suffer from inducing hypoglycemia. The stimulation of insulin secretion induced by prolonging the half-life of endogenous GLP-1 (as achieved with DPP IV inhibitors) is a more physiological approach to increase insulin secretion. The only therapeutic agent

Abbreviations: DPP, dipeptidyl-peptidase; GLP-1, glucagon-like peptide-1; GIP, glucose-dependent insulinotropic polypeptide; PO, prolyl oligopeptidase; *p*NA, para-nitroaniline; DTT, dithiothreitol

* Corresponding author. Tel.: +32 3 8202727; fax: +32 3 8202734.
E-mail address: anne-marie.lambeir@ua.ac.be (A.-M. Lambeir).

0006-2952/$ – see front matter © 2005 Elsevier Inc. All rights reserved.
doi:10.1016/j.bcp.2005.04.009

that has been demonstrated to reduce macrovascular events in type 2 diabetes, is metformin. As in several conditions, e.g. decreased renal or hepatic function, it is advised to stop metformin treatment, there is a need for new approaches to prevent the prolonged exposure of tissue to elevated glucose concentrations. Only this will limit the formation of advanced glycation end products that are thought to induce many of the vascular abnormalities [2].

Type 2 diabetes, also known as non-insulin dependent diabetes mellitus, is the most common form of diabetes. Incretins, such as glucagon-like peptide-1 (GLP-1) and glucose-dependent insulinotropic polypeptide (GIP), play an important role in normal and pathological blood glucose homeostasis. They are released from the gut in response to nutrient ingestion and promote nutrient assimilation via potentiation of glucose-dependent insulin secretion [3]. GLP-1 stimulates insulin secretion and biosynthesis and inhibits glucagon release when blood glucose levels are high. In addition, it appeared to regulate the growth and differentiation of the insulin-producing beta cells in the pancreatic islets in rodents [4]. In vitro and in vivo studies, using DPP IV and DPP IV-inhibitors, suggest that for GLP-1 and GIP, DPP IV truncation is the main degradation route [5]. One way by which the physiological effects of GLP-1 can be enhanced, is the use of DPP IV-inhibitors that will delay the degradation of this incretin [6,7].

Vildagliptin (NVP-LAF237/(2S)-{[(3-hydroxyadamantan-1-yl)amino]acetyl}-pyrrolidine-2-carbonitrile, structure in Scheme 1) [8] was described as a potent, selective and orally bio-available DPP IV-inhibitor. The compound was developed as a potential once daily therapeutic agent for type 2 diabetes [9]. In a phase I clinical study, Vildagliptin was administered to dietary-controlled type 2 diabetes patients, where it caused an increase in post-prandial active GLP-1 levels, a decrease in glucose levels and a reduction in the glucagon response to breakfast. Phase II clinical studies indicated that Vildagliptin was well tolerated. Liver enzymes were not changed; there was no significant change in body weight and a low incidence of hypoglycemic symptoms. Phase III safety and efficacy clinical trials were started in the first quarter of 2004 [10]. Because of its advanced state of development, Vildagliptin has become a reference compound against which new DPP IV inhibitors will need to be measured. Within this context we started the in vitro mechanistic study that is the subject of this paper.

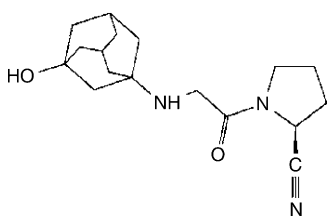

Scheme 1. Chemical structure of Vildagliptin.

Knowledge of the mechanism, the kinetics and the selectivity of an inhibitor may contribute significantly to a correct interpretation of its pharmacological properties and potential side effects. Tight binding inhibitors are important from a pharmacological point of view, because once bound to their target they inhibit the enzyme function even after the free drug has been cleared from the circulation or the specific site of action. Another important feature of an inhibitor is its selectivity. At least two human postproline dipeptidyl-peptidases, DPP 8 and DPP 9, whose functions are still unknown, are structurally closely related to DPP IV [11,12]. Lankas et al. [13] reported that the inhibition of DPP 8 in rats by an isoindoline containing compound gave rise to profound toxicity, including anemia, multiple histological pathologies and mortality. Minding these results, selective inhibition of DPP IV might be required for an acceptable safety and tolerability level of future antihyperglycemic agents of this type.

Screening and mechanistic investigation of DPP IV inhibitors is usually done by means of chromogenic or fluorogenic substrates, such as Gly-Pro-*p*-nitroanilide, Gly-Pro-4-methoxy-2-naphthylamide and Gly-Pro-aminomethylcoumarin. In these experiments, the S_2–S_1 substrate binding sites are occupied by the dipeptide part of the substrate. The leaving groups (*p*-nitroaniline, 4-methoxy-2-naphthylamine, aminomethylcoumarin) locate close to the S'_1 site. Inhibitor binding sites apart from S_2–S_1 and S'_1 are not probed using synthetic substrates. Peptidomimetic DPP IV-inhibitors are generally fairly small compounds which presumably interact in or close to the catalytic site. If long distance interactions with peptide substrates alter the conformation or the accessibility of the active site, the inhibition constants of certain inhibitors may be different when they are measured with a long peptide substrate rather than a peptide-derived synthetic substrate.

In this study, we addressed the interaction between Vildagliptin and purified human DPP IV, investigating the kinetics of binding and the type of inhibition. The selectivity with respect to other peptidases was explored. We determined the inhibitory potency on the DPP IV-catalyzed degradation of natural peptide substrates.

2. Materials and methods

2.1. Materials

Glycyl-prolyl-*p*-nitroanilide (Gly-Pro-*p*NA), alanyl-prolyl-*p*-nitroanilide (Ala-Pro-*p*NA), *N*-benzyloxycarbonyl-glycyl-prolyl-*p*-nitroanilide (Z-Gly-Pro-*p*NA), lysyl-prolyl-*p*-nitroanilide (Lys-Ala-*p*NA), GLP-1 and substance P were obtained from Bachem (Bubendorf, Switzerland). GIP, Tris, dithiothreitol (DTT) and EDTA were obtained from Sigma (St. Louis, MO), DMSO, acetonitrile, Hepes and potassium phosphate from Acros Organics (Geel, Belgium). Tween20 and sodium azide were from

Merck (Darmstadt, Germany). Vildagliptin was custom synthesized by GLSynthesis Inc. (Worcester, MA, USA).

2.2. Enzymes

Soluble DPP IV was purified from human seminal fluid as described before [14]. Porcine prolyl oligopeptidase was expressed in *E. coli* and purified using published methods [15]. Recombinant human DPP8 was expressed and purified as described [16]. Natural human DPP II was purified as reported [17]. Aminopeptidase N was enriched from human seminal plasma using DEAE-Sepharose FF anion-exchange, Sephacryl S300 HR gelfiltration, Q-sepharose Hiload ion exchange and (negative) anti-CD26 mAb-affinity chromatography. The specific activity of the aminopeptidase N preparation used in the experiments was 1 U/mg. Aminopeptidase P activity was measured in human platelet lysates without purification.

2.3. Caco2 cell culture

Human carcinoma colon (Caco2) cells provide a rich source of membrane bound DPP IV. The cells were maintained in Dulbecco's modified Eagle's essential medium supplemented with 1% nonessential amino acids, 20% foetal calf serum, 2 mM glutamine, penicillin (100 U/ml), streptomycin (100 μg/ml) and gentamycin sulfate (50 μg/ml) (GIBCO-BRL, Invitrogen, Carlsbad, CA). Cells from passage 30 were seeded in a 175 cm^2 flask and grown in 5% CO_2 at 37 °C. Medium was changed every 2 days until confluence was reached (6 days), from then on the medium was changed every day. Cells were harvested 10 days past confluence and lysed for 1 h in 100 mM Tris–HCl pH 7.5, 10 mM EDTA, 1/100 aprotinin and 1% octylglucopyranoside at 4 °C.

2.4. Activity measurements and IC_{50} determination

One unit of DPP IV activity is the amount of enzyme required to catalyze the conversion of 1 μmol of substrate per minute in presence of 0.5 mM Gly-Pro-*p*NA and 50 mM Tris buffer, pH 8.3 at 37 °C.

The IC_{50} is defined as the concentration of inhibitor required to obtain 50% reduction of the activity under specific assay conditions. The assay conditions for DPP IV were 50 mM Tris–HCl pH 8.3, 1 mM EDTA and 100 μM Gly-Pro-*p*NA; for DPP 8 the conditions were 50 mM Hepes pH 7.4, 0.1% Tween 20 and 300 μM Ala-Pro-*p*NA; for DPP II the conditions were 50 mM Cacodylic acid/NaOH pH 5.5 and 500 μM Lys-Ala-*p*NA. For PO the assay buffer was 0.1 M potassium phosphate pH 7.5, 1 mM DTT, 1 mM EDTA, 1 mM NaN_3 and 250 μM Z-Gly-Pro-*p*NA. Aminopeptidase N activity was measured using 300 μM Ala-*p*NA in 50 mM phosphate buffer pH 7.4. Aminopeptidase P activity was measured using 500 μM H-Lys(Abz)-Pro-Pro-*p*NA in 100 mM Tris–HCl, pH 7.5 containing 4 mM $MnCl_2$ [18].

The substrate concentrations were chosen near the K_m. Enzymes were preincubated with the inhibitor for 15 min at 37 °C. The reactions were started by addition of the appropriate substrate. Initial rates were measured by monitoring the absorbance at 405 nm in a final volume of 200 μl using the Spectramax340 (Molecular Devices, Sunnyvale, CA) microtiterplate reader, at 37 °C.

2.5. Slow-tight-binding inhibition curves and dissociation kinetics

The time dependency of DPP IV inhibition by Vildagliptin was measured under pseudo-first-order conditions by adding 160 μl DPP IV to 40 μl of a mixture of inhibitor and substrate and recording the release of free *p*NA at 405 nm using a Molecular Devices SpectraMax340 microtiterplate spectrophotometer. Progress curves were recorded using 2 U/l of DPP IV in 50 mM Tris–HCl, 1 mM EDTA, pH 8.3, at 37 °C. The final Gly-Pro-*p*NA concentrations ranged between 1 and 0.05 mM, the inhibitor concentrations were 250, 200, 150, 100, 50, 25 and 0 nM. The absorbance was measured every 5 or 10 s during 30 min or 1 h and blank absorbance values were subtracted from the data prior to subsequent calculations. Care was taken that no more than 10% of the substrate was converted during the reaction time. Data were exported into Microsoft Excel and curve fitting was performed using GraFit5 [19]. Data were fitted to the equation for slow binding inhibition [20]

$$A = A_o + \left((v_o - v_s) \frac{1 - \exp(-k_{obs} t)}{k_{obs}} \right) + v_s t \quad (1)$$

where A is the absorbance; v_o and v_s, the initial and final steady-state rates (expressed in A/time); t, time and k_{obs}, the observed pseudo first order rate constant of inhibitor binding.

Steady-state rates obtained from each progress curve were fitted against substrate and inhibitor concentrations using the rate equation for competitive inhibition

$$v_s = V_{max} \frac{[S]}{(K_m(1 + [I]/K_i)) + [S]} \quad (2)$$

and for mixed inhibition

$$v_s = \frac{V_{max}[S]}{K_m(1 + [I]/K_i) + [S](1 + [I]/K_i')} \quad (3)$$

by non-linear regression analysis. An F-test was preformed in order to determine the type of inhibition and the corresponding inhibition constants. The K_m for Gly-Pro-*p*NA was 100 μM.

In order to follow the dissociation of the Vildagliptin–DPP IV complex, aliquots of DPP IV were incubated without inhibitor and in the presence of 2.25 μM Vildagliptin at 37 °C. After 15 min the aliquots were diluted

100-fold into 0.5 mM Gly-Pro-*p*NA in 50 mM Tris–HCl, 1 mM EDTA, pH 8.3. The dissociation of the enzyme–inhibitor complex was monitored by substrate hydrolysis by measuring the absorbance every 10 s during 30 min.

2.6. Substrate decay curves

2.6.1. Gly-Pro-pNA

The time course of the complete degradation of Gly-Pro-*p*NA by DPP IV was measured in 50 mM Tris–HCl, 1 mM EDTA, pH 7.5, at 37 °C. The final substrate concentration was 5 μM. The inhibitor concentrations were 200, 150, 100, 50, 25, 10 and 2.5 nM. The reaction was started by adding 100 μl of DPP IV to 100 μl of a mixture of Gly-Pro-pNA and inhibitor. The final DPP IV concentration was 29 U/l. The release of *p*NA was followed at 405 nm every 10 s during 60 min. Blank absorbance values were subtracted from the data prior to subsequent calculations.

2.6.2. Substance P, GIP and GLP-1

To study the decay curves of peptide substrates (substance P, GIP and GLP-1), 70 μl of DPP IV was mixed with 70 μl of a solution containing substrate and inhibitor and incubated at 37 °C in presence of 50 mM Tris–HCl buffer, pH 7.5, 1 mM EDTA. The final DPP IV concentration was 29 U/l. The substrate concentration was 5 μM and Vildagliptin concentrations varied between 10 and 200 nM. At certain time intervals, 20 μl samples were withdrawn and quenched in 0.2% trifluoroacetic acid. C18 ZipTips (Millipore Corp., Bedford, MA) were used to desalt the samples. Elution was performed step-wise with 10 μl of 30 and 50% acetonitrile in 0.1% acetic acid. The composition of the mixture was determined with an Esquire ESI Ion Trap mass spectrometer (Bruker, Bremen, Germany). The instrument was used in a normal range, normal resolution setting, optimized on an *m*/*z* value near the most abundant ion of the intact peptide. The spectra were deconvoluted and the concentrations of the intact and truncated peptides were calculated from their relative abundance. The concentration of intact peptide was plotted against time. Peptide decay data were analyzed as a single exponential decrease and the in vitro $t_{1/2}$ was determined as described [21].

3. Results

3.1. Selectivity

In Table 1, we report the IC_{50} values of Vildagliptin obtained in standard conditions (see Section 2) using several sources of DPP IV and a number of potentially interfering proteases.

The IC_{50} of Vildagliptin for DPP IV was in the 100 nM range, irrespective whether purified DPP IV, human EDTA-plasma or Caco2-cell homogenates were used. Only DPP 8 was inhibited in this in vitro selectivity screening (IC_{50} of 9.0 ± 0.1 μM); the activity of DPP II, prolyl oligopeptidase, aminopeptidase P and aminopeptidase N was not significantly affected by Vildagliptin in the 0.1–1 mM concentration range.

Table 1
Selectivity of Vildagliptin for various enzymes

Enzyme source	IC_{50} (μM)
Dipeptidyl-peptidase IV	
Purified from human seminal fluid	0.120 ± 0.011
Caco2 cell lysate	0.117 ± 0.005
Human EDTA-plasma	0.102 ± 0.001
Recombinant human dipeptidyl-peptidase 8	9.0 ± 0.1
Dipeptidyl-peptidase II purified from human seminal fluid	>1000
Prolyl oligopeptidase	>1000
Aminopeptidase P in human platelet lysate	>100
Aminopeptidase N purified from human seminal plasma	>1000

The kinetic assays were performed as described in Section 2. Results are expressed as mean ± S.E.M (n = 3).

3.2. Kinetics of binding and dissociation

As illustrated in Fig. 1, the reaction progress curves in the presence of varied concentrations of Vildagliptin show a clear time and concentration dependent approach to the steady-state which is a characteristic of slow binding inhibition kinetics. The slow recovery of the enzymatic activity, after dilution of the pre-formed enzyme–inhibitor complex, proved that Vildagliptin was a reversible DPP IV inhibitor (Fig. 1, inset). The progress curves were fitted to

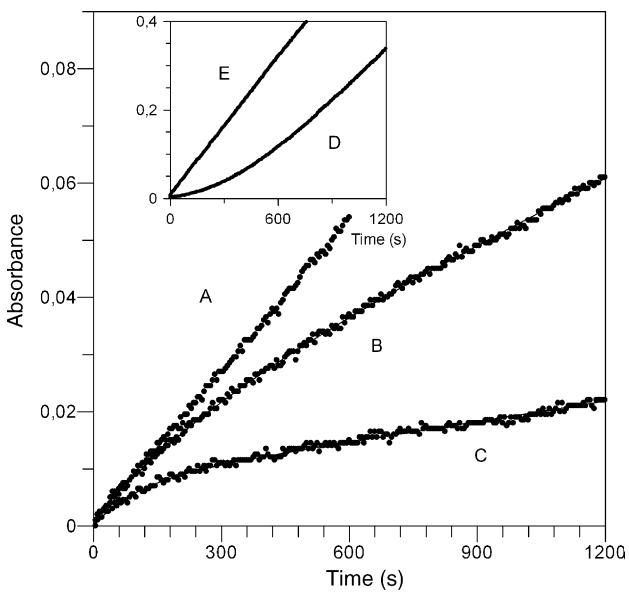

Fig. 1. Progress curves of Vildagliptin binding to DPP IV in presence of 0.1 mM Gly-Pro-*p*NA. The Vildagliptin concentrations were 0 (A), 50 (B) and 250 nM (C). The inset shows the dissociation of the Vildagliptin–DPP IV complex (D) after dilution to a final inhibitor concentration of 22.5 nM in presence of 0.5 mM Gly-Pro-*p*NA. Curve E is the control reaction in absence of inhibitor.

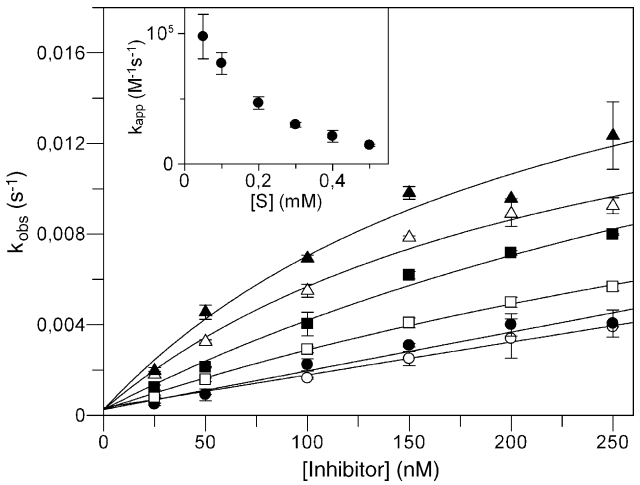

Fig. 2. Kinetic analysis of Vildagliptin binding to DPP IV. The observed pseudo-first order rate constants (k_{obs}) show a hyperbolic dependency upon the inhibitor concentration, indicative of a two step binding mode. The Gly-Pro-*p*NA concentrations were (▲) 0.05, (△) 0.1, (■) 0.2, (□) 0.3, (●) 0.4, and (○) 0.5 mM. The dependency of the apparent second order rate constant (k_{app}) on the substrate concentration is shown in the inset. This behavior is typical for a competitive inhibitor.

Eq. (1) to obtain values for k_{obs}, the observed pseudo first order rate constant for inhibitor binding. As shown in Fig. 2, there was a linear relationship between k_{obs} and the inhibitor concentration only at the higher substrate concentrations. At the lower substrate concentrations the dependency was hyperbolic. This behavior is often observed with slow-tight binding inhibitors and reflects a two-step binding mode.

$$E + \overset{K_1}{\rightleftarrows} EI \underset{k_{off}}{\overset{k_2}{\rightleftarrows}} EI^*$$

In the first step, the inhibitor forms a rather weak complex with the enzyme (EI) that is converted to the final high affinity EI^* complex in a rate limiting first order step. The hyperbolic curves of Fig. 2 reflect the saturation of the initial equilibrium. Because there was competition between the substrate and the inhibitor for the free enzyme, the apparent affinity of step 1 decreased when the substrate concentration increased. The expression for k_{obs} as a function of the inhibitor concentration is given by Eq. (4).

$$k_{obs} = k_{off} + k_2 \frac{[I]}{K_{1app} + [I]} \quad (4)$$

k_{off} is the overall dissociation rate constant; k_2, the first order rate constant of the slow second step; K_{1app}, the apparent dissociation equilibrium constant of the first step and [I], the total inhibitor concentration. The value of k_{off} could only be determined from the data points at 0.3–0.5 mM substrate, which lie on a straight line in Fig. 2. It is independent of the substrate concentration and was kept constant for the fitting of the hyperbolic curves with Eq. (4).

When $K_{1app} \gg [I]$, Eq. (4) becomes linear. This allows us to define an apparent second order rate constant, k_{app}.

Table 2
Comparison of the kinetic parameters for DPP IV inhibition by Vildagliptin and NVP-DPP728

	Vildagliptin	NVP-DPP728
K_i (nM)	17 ± 2	11 ± 4
k_{on} (10^5 M^{-1} s^{-1})	1.4 ± 0.5	1.3 ± 0.3
k_{off} (10^{-3} s^{-1})	2.5 ± 0.7	1.3 ± 0.2

Parameters were determined as in Figs. 2 and 3 from two independent experiments, each performed in duplicate. The errors are the S.E.M. k_{off} could not be accurately determined from the intercepts of the plots in Fig. 2, it was calculated using the $K_i = k_{off}/k_{on}$ equation. Parameters for NVP-DPP728 are from Hughes et al. [27].

For a competitive inhibitor the expression of this apparent second order rate constant is

$$k_{app} = \frac{k_2}{K_{1app}} = \frac{k_2}{K_1(1 + [S]/K_m)} \quad (5)$$

where K_1 is the dissociation equilibrium constant of the first step; K_m, the Michaelis constant of Gly-Pro-*p*NA and [S], the total substrate concentration. K_{1app} (>200 nM) and k_2 (approximately 0.02 s^{-1}) were difficult to determine from the plots in Fig. 2 because there were no data at saturating inhibitor concentrations. On the other hand, k_{app} could be determined more accurately from the slope or the tangent to the initial part of the hyperbolic plots. The substrate dependency of k_{app} was compatible with competitive inhibition (inset in Fig. 2). The substrate-independent second order rate constant ($k_{on} = k_2/K_1$) was obtained from the relationship expressed in Eq. (5).

The kinetic constants derived from experiments, such as in Fig. 2 are summarized in Table 2.

The K_i was calculated from the steady-state rates using the equation for competitive inhibition (Fig. 3, Table 2).

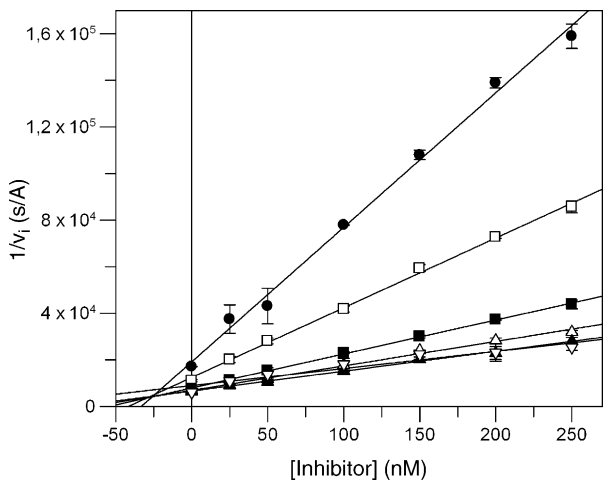

Fig. 3. Vildagliptin is a competitive inhibitor. The steady-state rates were measured in function of the substrate concentration at different Vildagliptin concentrations. The K_i was determined by fitting the data with the equation for competitive inhibition using a non-linear least squares program but here the data are shown as a Dixon plot. The K_i corresponds to the negative *X*-axis value of the intersection of the lines obtained at various substrate concentrations: (●) 0.05, (□) 0.1, (■) 0.2, (△) 0.3, (▲) 0.4, and (▽) 0.5 mM.

At first glance a K_i of 17 nM seems to be incompatible with the observed IC_{50} for DPP IV. However, as Vildagliptin is a slow binding inhibitor, special attention must be paid to how the IC_{50} value was obtained. As described in the experimental section, the enzyme was incubated with the inhibitor for 15 min prior to activity measurements. This time period is too short for the lower concentrations of inhibitor to equilibrate with the enzyme. The slow-binding kinetics might also explain the inconsistencies in the reported IC_{50} values [9,22].

3.3. Substrate decay curves

The reaction between DPP IV and natural peptides, and its inhibition by Vildagliptin, was followed by determining the composition of the reaction mixture at several time points using mass spectrometry. It was necessary to quantify the amount of peptide converted at various time points [21]. To achieve this the abundance signal of the mass spectrometer must be proportional to the concentration and this proportionality factor must be the same for the intact and truncated peptides. This was the case for GIP, with a mass of 4984.6 for the intact and 4750.4 for the truncated peptide. For GLP-1 masses of 3298.7 and 3089.9 were observed for the intact and the truncated peptide, respectively. The data from the decay of GIP and GLP-1 were analyzed as a single exponential decrease, where the concentration of intact peptide was plotted against the incubation time (Fig. 4).

The substance P mass spectra were less straightforward, mainly due to fragmentation of the peptides during analysis. For the intact peptide the native mass of 1347 was observed and also a fragment of mass 1200. The first truncation (SP-2) was characterized by molecules with mass of 1094 and 947, while the second truncation (SP-4) was characterized by masses 869 and 722. In addition, the reaction products and their fragments carried different charges as both truncations removed a dipeptide with a positive side chain (Arg-Pro, Lys-Pro) from substance P. Because an electron spray ionization type mass spectrometer was used, the various substance P fragments and degradation products were differently distributed in the mass spectra as 3+, 2+ and 1+ ions. Whereas it was relatively easy to calibrate the mass spectrometric abundance with mixtures of intact and fully truncated (SP-4) substance P, this was problematic with the intermediate form that does not accumulate during the reaction. The substance P decay curves were analyzed as consecutive reactions (Fig. 5). The decay of the intact form was described by a single exponential decrease. In absence of inhibitor the intermediate (SP-2) form was only transiently observed and the fully truncated (SP-4) form appeared after a typical lag time.

The effect of Vildagliptin on the in vitro truncation of the peptides is summarized in Table 3.

In absence of inhibitor the in vitro half-life is inversely proportional to the k_{cat}/K_m value of the peptide substrate (at a given enzyme concentration). The selectivity of DPP IV for substance P compared to GLP-1 and GIP can thus be deduced from the data in Table 3. The amount of inhibitor required to double the half-life of the peptide may be considered as an empirically defined IC_{50}. This experimental parameter may differ from the theoretical K_i due to the slow binding kinetics of Vildagliptin and competition with the substrate. Kinetic factors were important, certainly at the lower concentrations of the inhibitor. At 10 nM, the time required to reach equilibrium was approximately 25 min. This was obvious from the IC_{50} of the first truncation of substance P (25–100 nM range) compared to that of the second truncation (10–25 nM range). Competition with the substrate was probably not very important since the substrate concentration used (5 μM) was substantially lower than the reported K_m values for GIP, GLP-1 and substance P [23–26]. This is illustrated by the IC_{50} values determined with GIP and GLP-1, that were in the 10–25 nM range, similar to the K_i of 17 nM determined from the kinetic experiments using the chromogenic substrate.

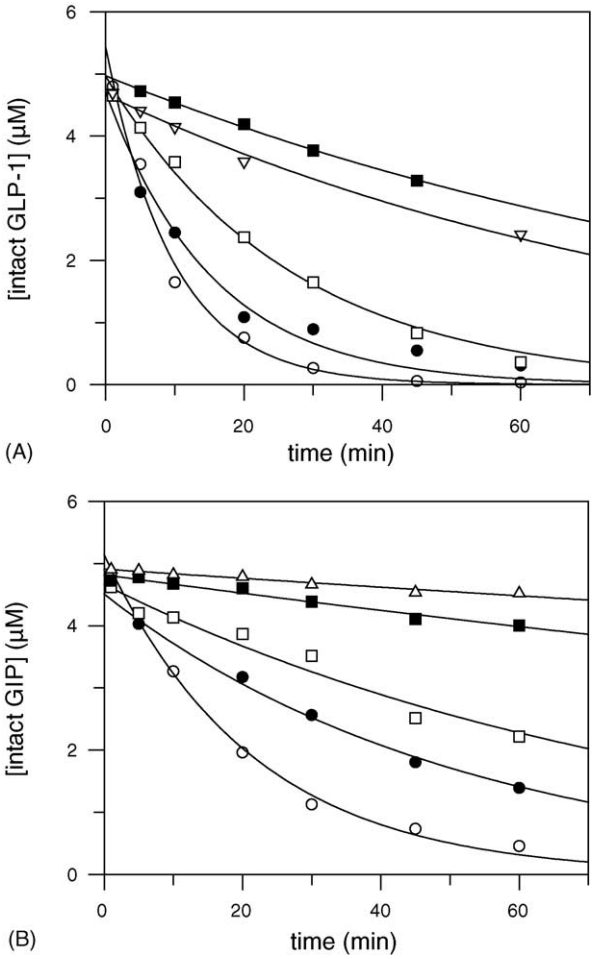

Fig. 4. Inhibition of DPP IV-catalyzed truncation of GIP and GLP-1. Decay of GLP-1 (A) and GIP (B) in presence of increasing concentrations of Vildagliptin: 0, 10, 25, 50 and 100 nM with GLP-1 and 0, 10, 25, 100 and 250 nM with GIP.

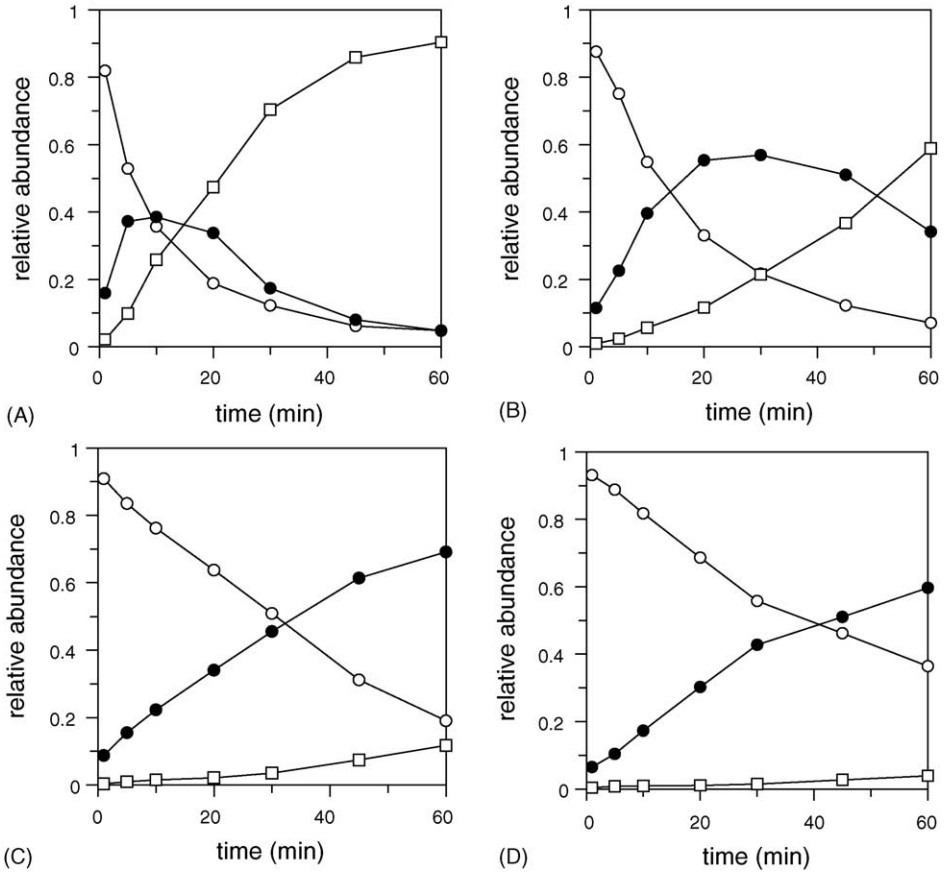

Fig. 5. Inhibition of DPP IV-catalyzed truncation of substance P. Truncation of substance P with 29 U/l DPP IV in presence of 0 nM (A), 25 nM (B), 100 nM (C) and 250 nM (D) Vildagliptin: (○) full-length substance P, (●) substance P after first truncation, (□) substance P after second truncation. The relative abundance is the abundance of the specified peptide divided by the sum of the abundances of all the observed peptides.

Also the time course of the conversion of the chromogenic substrate was followed in conditions identical to those used with the peptide substrates (Table 3). The decay curves of Gly-Pro-*p*NA in presence of Vildagliptin proved to be well suited to illustrate the effect of the slow-binding kinetics. The half-life of the chromogenic substrate is shorter than that of the peptides and the time required for the enzyme to equilibrate with the inhibitor is not at all negligible compared to $t_{1/2}$. In presence of Vildagliptin, the time course of *p*NA formation had two distinct phases: (1) the initial phase reflecting the disappearance of free enzyme into the EI^* complex and (2) the final phase where the substrate decayed exponentially as the free enzyme concentration remained constant (Fig. 6). When the $t_{1/2}$ was based only on the second phase, the IC_{50} value was 17 ± 1 nM, similar to the

Table 3
Half-life of substrates in the presence of DPP IV and Vildagliptin

	N-terminus	$t_{1/2}$ (min)							
		[Vildagliptin] (nM)							
		0	10	25	50	100	150	200	250
GIP	YAEGTFISD-	15 ± 1	35 ± 2	58 ± 6		217 ± 20 165 ± 27[a]			462 ± 31
GLP-1	HAEGTFTSD-	7 ± 1	11 ± 1 12 ± 1[a]	18 ± 1	36 ± 2	67 ± 5			
Substance-P	RPKPQQFFGLM	9 ± 1	11 ± 2	14 ± 1		30 ± 2 45 ± 2[a]			42 ± 1
SP-2	KPQQFFGLM	11 ± 3	12 ± 1	26 ± 4		>60			>60
Gly-Pro-*p*NA[b]		2.3 ± 0.2	3.4 ± 0.4	6 ± 1	11 ± 1	23 ± 3	36 ± 1	38 ± 6	

Half-lives were obtained from substrate decay curves, such as in Figs. 4–6. For GIP, GLP-1 and substance P the errors represent the standard error on the fit of the curves with a single exponential decay. For Gly-Pro-pNA the errors are the S.E.M. of two to five determinations.

[a] Inhibitor was preincubated with the enzyme for 15 min at 37 °C prior to addition of substrate.

[b] $t_{1/2}$ calculated from the time points where the inhibitor is in equilibrium with the enzyme.

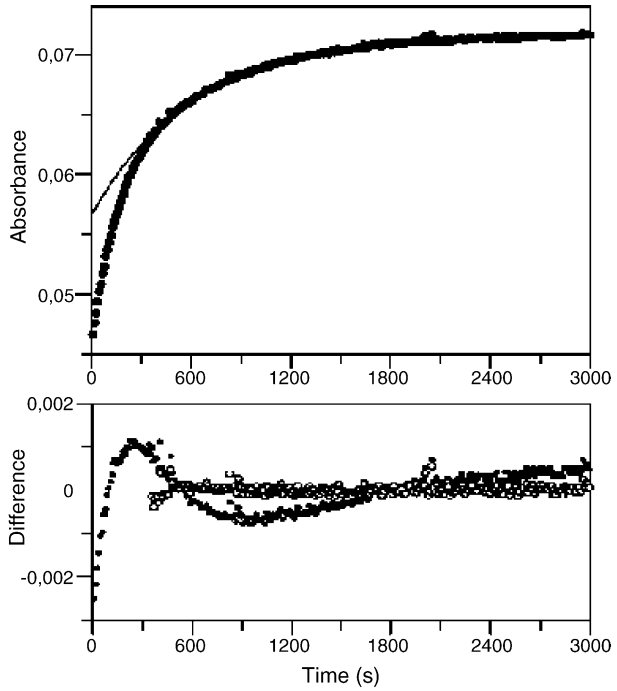

Fig. 6. Decay curve of 5 μM Gly-Pro-*p*NA in presence of 25 nM Vildagliptin. The absorbance increase due to *p*NA release occurs in two phases. Initially little inhibitor is bound and the reaction proceeds fairly fast. After approximately 10 min the equilibrium between DPP IV and Vildagliptin is reached and the substrate decay becomes exponential. In the lower panel the difference between the observed and fitted data points are plotted as a function of time. The closed circles represent the fit with a single exponential using all time points. The systematic deviation in the initial phase is large. The open circles represent the fit with a single exponential using only the time points of the second phase (curve shown in the top panel). In absence of inhibitor the substrate decay curves are exponential (data not shown).

values obtained with GIP, GLP-1 and the second cleavage of substance P.

In a separate experiment, GLP-1 and GIP were combined and incubated together with enzyme and inhibitor (25 nM). As shown in Fig. 7, the peptides were converted at different rates, consistent with their k_{cat}/K_m values. The relative increase in $t_{1/2}$ was the same for both substrates and similar to what was observed when they were incubated separately.

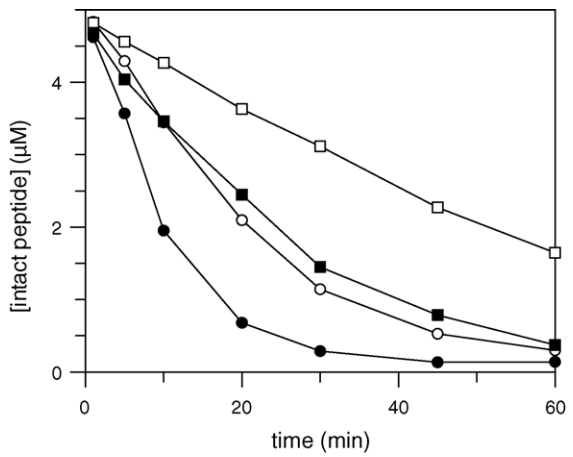

Fig. 7. Inhibition of the simultaneous truncation of GLP-1 and GIP by DPP IV. Decay curves are shown for GLP-1 (filled symbols) and GIP (open symbols) simultaneously incubated with 29 U/l DPP IV without inhibitor (circles) and in the presence of 25 nM Vildagliptin (squares).

4. Discussion

Vildagliptin was developed following a transition-state mimetic approach [9]. It belonged to a class of potent cyanopyrrolidine inhibitors in which a glycyl Xaa moiety was substituted with aliphatic and aromatic substituents. Hughes et al. [27] called these inhibitors remarkably specific for inhibition of DPP IV relative to other post-proline or post-alanine cleaving enzymes. The nitrile group on the pyrolidide ring of Vildagliptin proved to be very important for the high potency. Moreover, it turned out to be compatible with oral administration. The essential adamantyl group reduced the ability of the compound to cyclisize to its corresponding less active imidine derivative, an intermediate that could be formed by its predecessor, the less stable NVP-DPP728 [10,27,28]. As a candidate drug for a chronic illness, NVP-DPP 728 suffered from a short duration of action in vivo [9].

Vildagliptin is a slow-binding inhibitor, which inhibits DPP IV in a two step mechanism, as was reported for NVP-DPP728 [27]. We showed that Vildagliptin is a reversible, competitive inhibitor with association and dissociation rate constants similar to those published for NVP-DPP728 [27]. The K_i's of both inhibitors were also in the same range (Table 2).

During structure-activity relationship studies of large series of compounds, IC_{50} values are an excellent way of comparing the relative inhibitory potency. When IC_{50} values are reported, no assumptions are made concerning the mechanism of inhibition. The values usually depend upon the assay conditions which limits interlaboratory comparison. IC_{50} values between 2 and 4 nM were reported in the original study of NVP-LAF237 for DPP IV of different sources [9]. This is in the range of the K_i value determined in this study. In a counter-screening for DPP8 inhibitors, Jiaang et al. [22] published an IC_{50} of 51 nM for DPP IV and 14 μM for DPP8, similar to our data (Table 1).

The choice of peptidases for the selectivity studies was based on similarities with DPP IV concerning substrate selectivity and/or catalytic mechanism. The dipeptidyl peptidases II and 8 share with DPP IV a preference for substrates with a penultimate proline residue and prolyl oligopeptidase cleaves after a proline residue within a peptide chain. These three enzymes all belong to the prolyl oligopeptidase family within the clan SC of peptidases with serine type mechanism. Another peptidase included in the selectivity study was aminopeptidase N also known as CD13 which is, like DPP IV, a membrane bound enzyme.

Aminopeptidase P is a metalloproteinase that removes the N-terminal amino acid when there is a proline in second position.

The affinity of Vildagliptin for DPP8 was low compared to DPP IV. It is not known whether in vivo DPP8 is inhibited upon administration of therapeutic doses of Vildagliptin. Acute toxicity in animal models was reported for at least one compound with strong DPP8/9 inhibitory potency [13]. To date no in vivo effects of Vildagliptin were reported that point to a pharmacological impact of the inhibition of other peptidases.

First reports on the safety profile of Vildagliptin are very promising but as is the case for all new pharmacological agents, additional studies are needed to obtain a thorough insight in the in vivo effects of DPP IV inhibition [4,10]. The involvement of DPP IV in the in vivo metabolism of different peptides may open new pharmaceutical opportunities for DPP IV inhibitors or may form the basis for side-effects. Many peptides have been described as DPP IV substrates in vitro; for only a few this role has been confirmed in vivo (reviewed in [1]). For the in vitro study of Vildagliptin action in presence of natural peptides we chose GLP-1 and GIP since they are the physiological target and their catalytic parameters (with DPP IV) were previously reported [23–25]. GLP-1 and GIP are somewhat atypical DPP IV substrates, as they are cleaved after an alanine instead of a proline. In vivo effects (unrelated to glucose homeostasis) of DPP IV truncation have been reported for a number of peptides that are cleaved after proline, including several chemokines, neuropeptide Y and substance P [21,26]. Substance P was chosen in the present study as a representative of Xaa-Pro containing peptide substrates. Preliminary results with SDF-1alpha indicated that the truncation of this chemokine is also efficiently inhibited by Vildagliptin in vitro (data not shown). The methods described here may be used to investigate hypotheses of substrate specific inhibition by other inhibitors in presence of other interesting DPP IV substrates, such as glucagon.

The crystal structures of DPP IV in complex with substrates and inhibitors provide some insight in how relatively short peptides bind in the active site [29–33]. However, there is only limited information on how larger peptides, for example incretins and chemokines, interact with the enzyme. This has led to some speculation concerning, for example, the role of the beta-propeller domain in controlling the access to the active site and the exact route of entry to the active site. From kinetic experiments with natural peptide substrates, inhibition experiments with oligopeptides and equilibrium binding experiments with GLP-1, there is some evidence for long-range interactions between peptides and DPP IV [21,34–37]. For example, the great efficiency of cleavage after the penultimate alanine by DPP IV of peptides, such as GLP-1 and GIP compared to dipeptide-derived alanine containing chromogenic substrates may be an indication that extended substrate interactions are used to stabilize the transition state of the hydrolysis of these peptide substrates. These considerations and rumors of half-of-the-site activity and allosteric interactions by peptide sequences have fuelled the concern that screening of lead compounds with small chromogenic or fluorogenic substrates may be insufficient to develop an efficient and ''substrate-selective'' DPP IV inhibitor. In the results presented in this paper there was no evidence for substrate specific inhibition of DPP IV by Vildagliptin or of important allosteric factors affecting the inhibition constant in presence of GIP and GLP-1. When GIP and GLP-1 are presented simultaneously to DPP IV, they are degraded at rates proportional to their k_{cat}/K_m values as expected for competing substrates. The truncation of both peptides is inhibited to the same extent. These observations are in full agreement with the competitive behavior of Vildagliptin: it acts by reducing the amount of free enzyme available for substrate hydrolysis.

Acknowledgements

This work was supported by the Fund for Scientific Research Flanders-Belgium (F.W.O.-Vlaanderen). I. Brandt and M.B Maes are research assistants from the F.W.O.-Vlaanderen. J. Joossens is a fellow of the Institute for the Promotion of Innovation through Science and Technology in Flanders (I.W.T.-Vlaanderen).

References

[1] Lambeir AM, Durinx C, Scharpé S, De Meester I. Dipeptidyl-peptidase IV from bench to bedside: an update on structural properties, functions, and clinical aspects of the enzyme DPP IV. Crit Rev Clin Lab Sci 2003;40:209–94.

[2] Davis SN, Granner DK. Insulin, oral hypoglycemic agents and the pharmacology of the endocrine pancreas. In: Hardman JG, Limbird LE, editors. The pharmacological basis of therapeutics. 10th ed. Mcgraw-Hill; 2001. p. 1679–714.

[3] Drucker JD. Therapeutic potential of dipeptidyl peptidase IV inhibitors for the treatment of type 2 diabetes. Expert Opin Invest Drugs 2003;12:87–100.

[4] Weber A. Dipeptidyl peptidase IV inhibitors for the treatment of diabetes. J Med Chem 2004;47:4135–41.

[5] Mentlein R. Dipeptidyl peptidase IV (CD26)-role in the inactivation of regulatory peptides. Regul Pept 1999;85:9–24.

[6] Ahrén B, Landin-Olsson M, Jansson PA, Svensson M, Holmes D, Schweizer A. Inhibition of dipeptidyl peptidase-4 reduces glycemia, sustains insulin levels, and reduces glucagon levels in type 2 diabetes. J Clin Endocrinol Metab 2004;89:2078–84.

[7] Deacon CF, Ahrén B, Holst JJ. Inhibitors of dipeptidyl peptidase IV: a novel approach for the prevention and treatment of Type 2 diabetes? Expert Opin Invest Drugs 2004;13:1091–102.

[8] International nonproprietary names for pharmaceutical substances (INN), recommended international nonproprietary names: list 52 WHO Drug information 2004;18:263.

[9] Villhauer EB, Brinkman JA, Naderi G, Burkey BF, Dunning BE, Prasad K, et al. 1-[[(3-Hydroxy-1-adamantyl)amino]acetyl]-2-cyano-(S)-pyrrolidine: a potent, selective, and orally bioavailable dipeptidyl

peptidase IV inhibitor with antihyperglycemic properties. J Med Chem 2003;46:2774–89.
[10] Barlocco D. LAF-237. Curr Opin Invest Drugs 2004;5:1094–100.
[11] Abbott CA, Yu DM, Woollatt E, Sutherland GR, McCaughan GW, Gorrel MD. Cloning, expression and chromosomal localization of a novel human dipeptidyl peptidase (DPP) IV homolog, DPP8. Eur J Biochem 2000;267:6140–50.
[12] Olsen C, Wagtmann N. Identification and characterization of human DPP9, a novel homologue of dipeptidyl peptidase IV. Gene 2002;299: 185–93.
[13] Lankas G, Leiting B, Roy RS, Eiermann G, Biftu T, Kim D, et al. Inhibition of DPP8/9 results in toxicity in preclinical species: potential importance of selective dipeptidyl peptidase IV inhibition for the treatment of Type 2 DM. Diabetes 2004;53(Suppl. 2):A2. 7-OR.
[14] De Meester I, Vanhoof G, Lambeir AM, Scharpé S. Use of immobilized adenosine deaminase (EC 3.5.4.4) for the rapid purification of native human CD26/dipeptidyl peptidase IV (EC 3.4.14.5). J Immunol Methods 1996;189:99–105.
[15] Szeltner Z, Renner V, Polgar L. Substrate- and pH-dependent contribution of oxyanion binding site to the catalysis of prolyl oligopeptidase, a paradigm of the serine oligopeptidase family. Protein Sci 2000;9:353–60.
[16] Chen YS, Chien CH, Goparaju CM, Hsu JTA, Liang PH, Chen X. Purification and characterization of human prolyl dipeptidase DPP8 in Sf9 insect cells. Protein Expr Purif 2004;35:142–6.
[17] Maes MB, Lambeir AM, Gilany K, Senten K, Van der Veken P, Leiting B, et al. Kinetic investigation of human dipeptidyl peptidase II (DPPII)-mediated hydrolysis of dipeptide derivatives and its identification as quiescent cell proline dipeptidase (QPP)/dipeptidyl peptidase 7 (DPP7). Biochem J 2005;386:315–24.
[18] Stockel-Maschek A, Stiebitz B, Koelsch R, Neubert K. A continuous fluorimetric assay for aminopeptidase P detailed analysis of product inhibition. Anal Biochem 2003;322:60–6717.
[19] Leatherbarrow RJ. GraFit Version 5. Horley, UK: Erithacus Software Ltd; 2001.
[20] Venäläinen JI, Juvonen RO, Garcia-Horsman JA, Wallén EAA, Christiaans JAM, Jarho EM, et al. Slow-binding inhibitors of prolyl oligopeptidase with different functional groups at the P1 site. Biochem J 2004;382:1003–8.
[21] Lambeir AM, Durinx C, Proost P, Van Damme J, Scharpé S, De Meester I. Kinetic study of the processing by dipeptidyl-peptidase IV/CD26 of neuropeptides involved in pancreatic insulin secretion. FEBS Lett 2001;507:327–30.
[22] Jiaang WT, Chen YS, Hsu T, Wu SH, Chien CH, Chang CN, et al. Novel isoindoline compounds for potent and selective inhibition of prolyl dipeptidase DPP8. Bioorg Med Chem Lett 2005;15:687–91.
[23] Mentlein R, Gallwitz B, Schmidt WE. Dipeptidyl-peptidase IV hydrolyses gastric inhibitory polypeptide, glucagon-like peptide-1(7-36)amide, peptide histidine methionine and is responsible for their degradation in human serum. Eur J Biochem 1993;214:829–35.
[24] Pauly RP, Rosche F, Wemann M, McIntosh CH, Pederson RA, Demuth HU. Investigation of glucose-dependent insulinotropic polypeptide-(1-42) and glucagon-like peptide-1-(7-36) degradation in vitro by dipeptidyl peptidase IV using matrix-assisted laser desorption/ionization-time of flight mass spectrometry. J Biol Chem 1996;271: 23222–9.
[25] Kikuchi M, Fukuyama K, Epstein WL. Soluble dipeptidyl peptidase IV from terminal differentiated rat epidermal cells: purification and its activity on synthetic and natural peptides. Arch Biochem Biophys 1998;266:369–76.
[26] Naush I, Heymann E. Substance P in human plasma is degraded by dipeptidyl peptidase IV, not by cholinesterase. J Neurochem 1985; 44:1354–7.
[27] Hughes TE, Mone MD, Russell ME, Weldon SC, Villhauer EB. NVP-DPP728 (1-[[[2-[5-Cyanopyridin-2-yl)amino]ethyl]amino]acetyl]-2-cyano-(S)-pyrrolidine), a slow-binding inhibitor of dipeptidyl peptidase IV. Biochemistry 1999;38:11597–603.
[28] Augustyns K, Van der Veken P, Senten K, Haemers A. Dipeptidyl peptidase IV inhibitors as new therapeutic agents for the treatment of Type 2 diabetes. Expert Opin Ther Patents 2003;13:1–12.
[29] Hiramatsu H, Yamamoto A, Kyono K, Higashiyama Y, Fukushima C, Shima H, et al. The crystal structure of human dipeptidyl peptidase IV (DPP IV) complex with diprotin A. Biol Chem 2004;385:561–4.
[30] Oefner C, D'Arcy A, Mac Sweeney A, Pierau S, Gardiner R, Dale GE. High-resolution structure of human apo dipeptidyl peptidase IV/CD26 and its complex with 1-[([2-[(5-iodopyridin-2-yl)amino]-ethyl]amino)-acetyl]-2-cyano-(S)-pyrrolidine. Acta Crystallogr D Biol Crystallogr 2003;59:1206–12.
[31] Aertgeerts K, Ye S, Tennant MG, Kraus ML, Rogers J, Sang BC, et al. Crystal structure of human dipeptidyl peptidase IV in complex with a decapeptide reveals details on substrate specificity and tetrahedral intermediate formation. Protein Sci 2004;13:412–21.
[32] Rasmussen HB, Branner S, Wiberg FC, Wagtmann N. Crystal structure of human dipeptidyl peptidase IV/CD 26 in complex with a substrate analog. Nat Struct Biol 2003;10:19–25.
[33] Engel M, Hoffmann T, Wagner L, Wermann M, Heiser U, Kiefersauer R, et al. The crystal structure of dipepidyl peptidase IV (CD26) reveals its functional regulation and enzymatic mechanism. Proc Natl Acad Sci USA 2003;100:5063–8.
[34] Lambeir AM, Proost P, Durinx C, Bal G, Senten K, Augustyns K, et al. Kinetic investigation of chemokine truncation by CD26/dipeptidyl peptidase IV reveals a striking selectivity within the chemokine family. J Biol Chem 2001;276:29839–45.
[35] Zhu L, Tamvakopoulos C, Xie D, Dragovic J, Shen X, Fenyk-Melody JE, et al. The role of dipeptidyl peptidase IV in the cleavage of glucagon family peptides: in vivo metabolism of pituitary adenylate cyclase activating polypeptide-(1-38). J Biol Chem 2003;278:22418–23.
[36] Lorey S, Stockel-Maschek A, Faust J, Brandt W, Stiebitz. Gorrell MD, et al. Different modes of dipeptidyl peptidase IV (CD26) inhibition by oligopeptides derived from the N-terminus of HIV-1 Tat indicate at least two inhibitor binding sites. Eur J Biochem 2003;270:2147–56.
[37] Hinke SA, Kuhn-Wache K, Hoffmann T, Pederson RA, McIntosh CH, Demuth HU. Metformin effects on dipeptidylpeptidase IV degradation of glucagon-like peptide-1. Biochem Biophys Res Commun 2002; 291:1302–8.